Crimson Publishers
Wings to the Research

Research Article

Corrosion Monitoring of Austenitic and Super Austenitic Stainless-Steel Coupons in a Biodiesel Plant

CEAS Torres[1], TE Santos[2] and VFC Lins[2]*

[1]Petrobras, Avenida das Indústrias 531, Brazil

[2]Chemical Engineering Department, Brazil

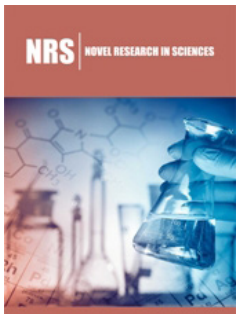

Abstract

Corrosion monitoring of austenitic stainless steels was performed in a biodiesel plant by using corrosion coupons due to the generalized corrosion observed in stainless steel. Corrosion resistance of AISI 304L, AISI 316L, AISI 317L and AISI 904L stainless steels was evaluated downstream of the hydrochloric acid insertion site in the biodiesel and glycerin streams, between static mixer and decanter (biodiesel circuit point 1) and between static mixer and a heat exchange (in glycerin circuit point 2). AISI 317L presented a good corrosion resistance at monitoring point number 1. At monitoring point 2, AISI 317L steel performed better than AISI 904L. AISI 317L was selected as pipe material to be used downstream of the insertion point of the hydrochloric acid solution into the biodiesel and glycerin stream.

Keywords: Corrosion monitoring; Corrosion coupons; AISI 316L steel; AISI 317L steel; Biodiesel plant

***Corresponding author:** VFC Lins, Corrosion and Surface Engineering Laboratory, Chemical Engineering Department, Federal University of Minas Gerais, Brazil

Submission: November 21, 2019

Published: December 06, 2019

Volume 2 - Issue 5

How to cite this article: CEAS Torres1, TE Santos2 and VFC L. Lattice Dilation of Plasma Sprayed Nickel Film Quantified by High Resolution Terahertz Imaging. Nov Res Sci.2(5). NRS.000546.2019.
DOI: 10.31031/NRS.2019.2.000546

Introduction

Biodiesel is one of the alternative fuels researched to replace petroleum derivatives [1]. A reaction between the triglyceride (vegetal oil or adipose) and alcohol (methanol) with an alkaline catalyst occurs at 64 °C, at atmospheric pressure, and is accompanied by sedimentation, neutralization, washing, distillation and filtration resulting in a biodiesel product and a glycerine co product specified [2]. Alkali-catalysed transesterification is a most commonly used process for oils with low free fatty acids and low moisture content [2]. The neutralization of catalysts with hydrochloric acid is an important step in the biodiesel process that can generate steel corrosion due to the very low pH [3]. In a Brazilian biodiesel plant, the most used material in equipment and piping in the transesterification region is the AISI 316L stainless steel (SS). The corrosion of steel equipment is a major problem in biofuel plants. The failures, which occur due to corrosion, impair the operational reliability which causes production and economic losses.

Corrosion of SS in media containing chlorides is extensively studied in literature [4-8]. Chloride-induced pits are enriched in chloride ions, which are attracted by metal cations produced, or show a lower pH relative to the bulk solution in order to maintain the active dissolution of metal [9-12]. Local acidification also occurs as a result of hydrolysis of the dissolving metal cations within the anolyte [9-12].

Monitoring corrosion rates of SS, in very specific media, which contain chlorides, but consist of an acidified glycerine and processed biodiesel was not found in literature, to the best of our knowledge. Corrosion monitoring was performed at a temperature of 64 °C, in situ in a biodiesel industrial plant, where the stainless steels were also subject to a generalized corrosion with mass loss. Biodiesel has been found to be more corrosive to automotive materials than diesel [13-17]. The corrosive characteristic of biodiesel can be due to the presence of oxygen moieties, auto-oxidation, increased polarity of biodiesel and its hygroscopic nature. Corrosion of different metals such as copper, brass, bronze, cast iron, and carbon steel in diesel and biodiesel was investigated by several researchers [13-17], but corrosion resistance of austenitic SS in fluids of a biodiesel plant such as processed biodiesel and acidified glycerine was not found in literature.

In this work, results of corrosion monitoring by steel coupons were presented and discussed. The identification of the main failures contributed to select the monitoring points for installation of corrosion coupons. As the failure cases were associated to the AISI 316L SS, the steels selected as corrosion coupons were the AISI 316L SS, more corrosion resistant steels (AISI 317L and 904L) and one less corrosion resistant steel (AISI 304L SS) than the AISI 316L SS.

Methodology

Fluid characterization

Two major points were selected for the collection of samples: one for biodiesel (at the input of the decanter) and the other for glycerine (on input of heat exchanger), both downstream from the acid dosing hydrochloric acid. With the stable load of 11,000kg/h, ten samples of each fluid were collected applying two-hour intervals between each collection. The process fluids were characterized in terms of moisture, conductivity and pH, which represent the environment of at least 70% of the points where faults occurred by corrosion. The biodiesel samples were collected at the input of the second settling tank, while the glycerine samples were collected at the inlet of the heat exchanger. The DM-32 Digimed conductivity measurement equipment and a Digimed pH meter Model DM-22 were used to measure the conductivity and the pH of the fluids. The moisture measurement was performed according to the ASTM E 203 (2008) Standard.

Corrosion coupons

The procedure adopted for the implementation of the corrosion monitoring system in the unit followed the guidelines in the NACE RP-0775 (2005) and ASTM G1-3 (2011) Standards. Forty-five circular coupons of AISI 304L, AISI 316L, AISI 317L, and AISI 904L were used; shaped from a rolled sheet, which was kindly supplied by the Sandvik Company.

The chemical composition of the steels is shown in Table 1. The diameter of the central hole of the spherical coupons was 5.23mm, the total diameter was 19.10mm and the thickness were 2.43mm. The coupons were mounted on Metal Samples Corrosion Monitoring Systems door coupons; LP2100 model, with plug 25.4mm NPT thread, stainless steel body AISI 316, maximum insertion length of 175.77mm, and a retractable safety chain that allowed insertion and removal of the coupons while the unit was in operation. To minimize the interference in the process, the corrosion testers were installed in a position tangent to the equipment wall, as shown in Figure 1. The operating temperature and maximum pressure were 260 °C and 10.2MPa. Two points of corrosion monitoring were selected as shown in Figure 2 and 3, in Table 2.

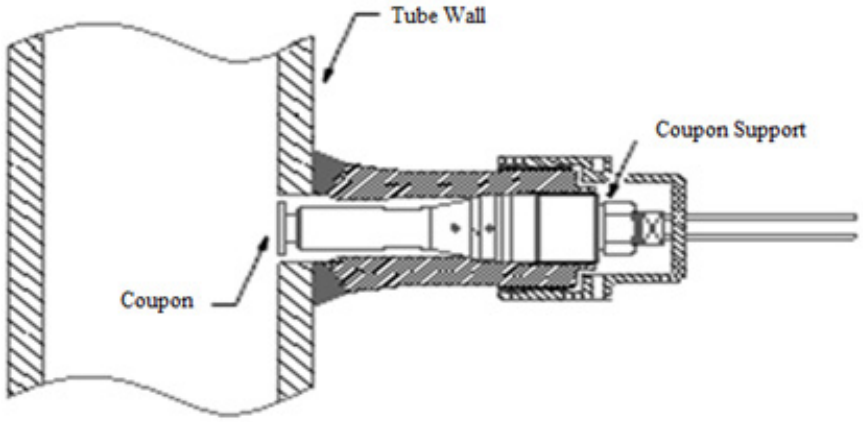

Figure 1: Installation position of coupons in pipes.

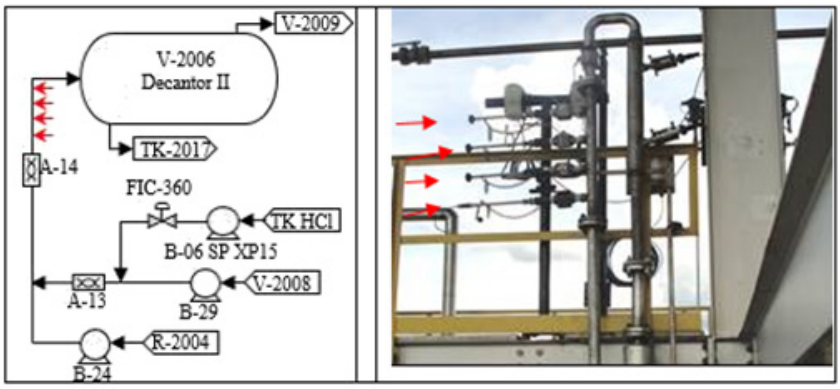

Figure 2: Monitoring point 1.

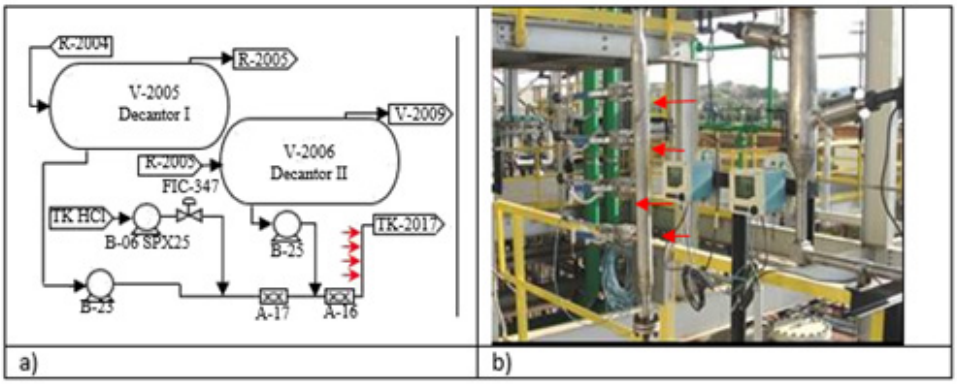

Figure 3: Monitoring point 2.

Table 1: Chemical composition (wt.%) and PREN of steels.

AISI	C	Cr	Ni	Mo	N	PREN
304L	0.03	19.01	10.2	0	0.1	20.61
316L	0.03	16.46	9.99	2.03	0.1	24.76
317L	0.03	18	13	3.5	0.1	31.15
904L	0.02	19.99	24.57	4.22	0.1	35.52

Table 2: Corrosion monitoring points.

1	Between static mixer A-2014 and decanter V-2006 Process biodiesel in neutralization (downstream of the hydrochloric acid dosage), 69 °C, pH 4.5 - 6.5, mass flow of 8.5 - 15.0t/h, coupons of AISI 304L, 316L, 317L, and 904L
2	Between static mixer A-2016 and P-22 heat exchanger, Process glycerin (downstream of the hydrochloric acid dosage) 69 °C, pH 4.0 - 5.5, mass flow of 1.6 - 2.4t/h, coupons of AISI 304L, 316L, 317L, and 904L

Corrosion coupons were stored in a non-metallic container, wrapped with cotton wool and silica gel for moisture absorption. Handling of coupons was performed with gloves to prevent oxidation and contamination by handling. Coupons were identified and cleaned with acetone before initial weighing. Mass measurements of dried coupons were performed using a Sartorius analytical scale CPA324S model with measurement uncertainty of ±0.1mg. Dimensions of the coupons were measured with a calliper (uncertainty ±0.05mm) to determine the exposed area, discounting the area covered by the fixation device in the coupon holder. Coupons were photographed before installation. The coupons were mounted on carriers and the electrical insulation was checked with multimeter. Coupon holders were installed in the process, recording the location, the control number, the date and time of the installation. Operational parameters were monitored, recording abnormalities that may influence the corrosive process. After set exposure period, the coupon was removed, photographed and cleaned using neutral detergent to remove oily residues. Corrosion products were removed by immersing the coupons for 20min in 10vol.% nitric acid solutions in distilled water at 60 °C. Coupons were cleaned with neutral detergent and rinsed with distilled water. Mass measurements of dried coupons were performed using a Sartorius analytical scale, CPA324S model with measurement uncertainty of ±0.1mg. Visual observation of coupons was performed, and corrosion coupons were photographed.

Results and Discussion

The average moisture of biodiesel is 3.6%, conductivity is 1μS/cm, and pH was 4. The average moisture of processed glycerine samples was 17.3%. The conductivity of glycerine was 14,000S/cm, and all glycerine samples showed a pH equal to 6. The AISI 304L, AISI 316L, AISI 317L and AISI 904LSS were evaluated in five different campaigns at the monitoring point 01 (A-14) downstream of the hydrochloric acid insertion site in the biodiesel stream. In the last two campaigns, AISI 304L steel was replaced by AISI 317L steel.

The performance of AISI 304L was substantially lower than the other performances, with a mean corrosion rate of 0.4001mm/year, 17 times higher than the corrosion rate presented by AISI 316L and 115 times higher than the corrosion rate presented by the AISI 904L. AISI 317L showed a good performance, presenting an average corrosion rate of 0.0007mm /year, 7 times lower than the corrosion rate presented by AISI 316L, and close to the corrosion rate presented by AISI 904L.

AISI 316L and AISI 904L steels presented low corrosivity potential, considering that in both, the corrosion rate was lower than 0.025mm/year. The corrosion rate presented by AISI 904L was 7 times lower than the corrosion rate presented by AISI 316L, proving the greater nobility of the material. Table 3 shows the

corrosion rates of the coupons installed at monitoring point 1 (A-14), segregated by campaign and by steel. A clear reduction of the corrosion rate of AISI 316L steel from the first to the third campaign, with subsequent stabilization, was observed. This reduction is related to the optimization of the hydrochloric acid dosing system during the development of this research project, which also showed a repercussion on the reduction of the rate of corrosion failure. Figure 4 shows coupons after removal from the monitoring point 1.

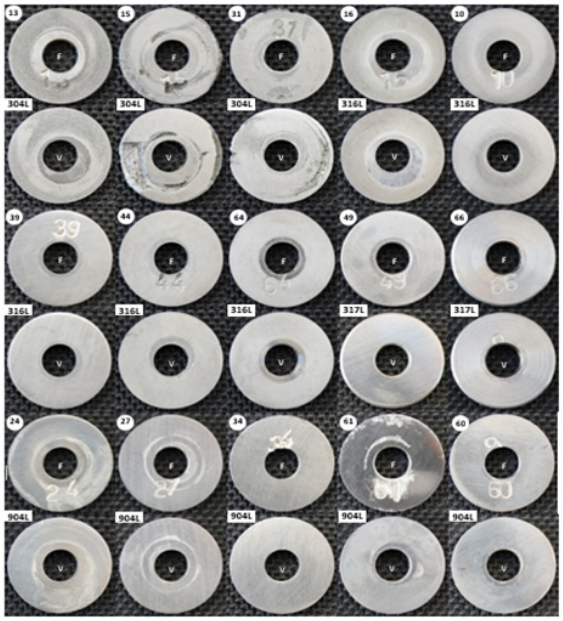

Figure 4: Corrosion coupons after removal from monitoring point 1.

Table 3: Corrosion rates (mm/year) of coupons installed in monitoring point number 1.

	C1	C2	C3	C4	C5	Average (C1 –C3)	Average (C4-C5)	Total average
AISI 304L	0.541	0.5801	0.0791	------	-------	0.4001	-------	0.4001
AISI 316L	0.0521	0.0138	0.0044	0.0046	0.0048	0.0234	0.0047	0.0159
AISI 317L	----	------	-------	0.0003	0.001	------	0.0007	0.0007
AISI 904L	0.0025	0.006	0.0019	0.0003	0.0001	0.0035	0.0002	0.0022

AISI 304L, 316L, 317L and 904L SS were evaluated downstream of the insertion point of the hydrochloric acid solution into the glycerine stream, monitoring point 2 (A-16). In the last two campaigns, AISI 304L steel was replaced by AISI 317L steel.

The performance of AISI 304L was again much lower than the others, with a mean corrosion rate of 0.4790mm/year, 33 times higher than the corrosion rate presented by AISI 316L and 103 times higher than the corrosion rate presented by AISI 904L. Diverging from the theoretical domain, the AISI 317L steel performed nobler than AISI 904L, presenting a 52% lower corrosion rate in the average of the campaigns in which they were tested simultaneously. The AISI 904L steel contains a higher Mo content (4.22wt.%) than the AISI 317L steel (3.50wt.%). Literature [18] reported the beneficial effect of molybdenum on localized corrosion resistance of austenitic stainless steels, mainly in media containing chlorides. Upadhyay et al. [18] observed higher pitting potentials for austenitic stainless steels with higher Mo contents. In this work, they identified the presence of Mo oxides, Cr enrichment (through various Cr spinels), and polymolybdates in the passive films of 316LN and 317LNSSs, which imparted increased pitting resistance to these steels in relation to the AISI 304L without Mo addition. Cutler and Coates [19] reported that if localized corrosion

of austenitic stainless steels does occur, nickel is effective in decrease the propagation rate of corrosion. The corrosion mechanisms that operate in this research are related to the effect of the higher contents of molybdenum and nickel in the austenitic steels, especially in the super austenitic steels that increase the corrosion resistance of the steels, especially in aggressive media as in the media containing chlorides. In this way, the steel more resistant to corrosion should be the super austenitic that presents the highest levels of molybdenum, nickel and chromium. However, in the specific industrial conditions of the biodiesel plant, an interesting result obtained was that molybdenum contents of 3.50wt.% and nickel of 13wt.% were sufficient to assure a satisfactory corrosion resistance in the studied medium.

AISI 316L and AISI 904L steels presented low corrosivity potential, considering that in both steels the corrosion rate was lower than 0.025mm /year. The corrosion rate presented by the AISI 904L was 55% lower than the corrosion rate presented by the AISI 316L, proving the greater nobility of the material. Table 4 shows the corrosion rates of the coupons installed at monitoring point 02 (A-16), segregated by campaign and by material. It can be observed, in campaigns 4 and 5, the relatively close performance of AISI 316L, AISI 317L and AISI 904L SS.

Table 4. Corrosion rates (mm/year) of steel coupons installed. The post-exposure state of the mass loss coupons (front-F and V-back) installed at monitoring point 2 is shown in Figure 5. Coupon 22, which recorded the highest corrosion rate in the tests, presented severe corrosion with characteristics of the generalized form. In coupon 5, a localized attack occurred, with characteristics of the alveolar, pitting and cracks (under the coupon holder insulation ring). The tags observed in coupons 58 and 59 are related to acid etching, post exposure, for oxide removal, and not to the development of corrosive process, as attested by the low recorded corrosion rates.

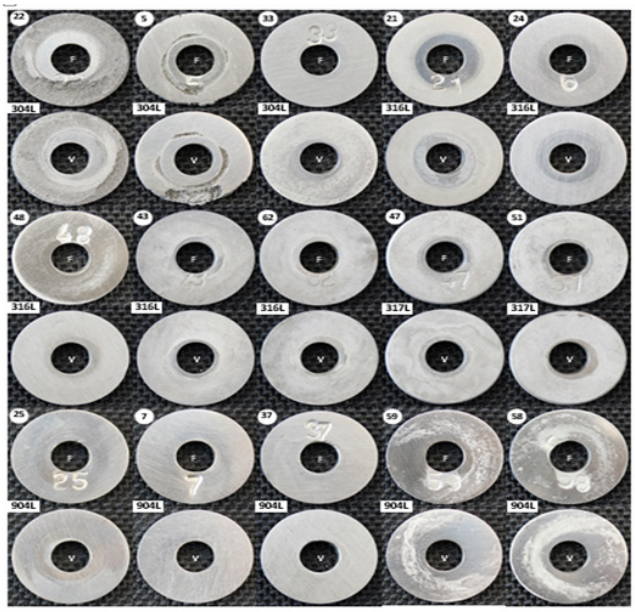

Figure 5: Post-exposure state of the mass loss coupons (front-F and V-back) installed at monitoring point 2.

Table 4: Corrosion rates (mm/year) of steel coupons installed at monitoring point 2.

	C1	C2	C3	C4	C5	Average (1-3_	Average (4,5)	Total average
AISI 304L	1.0158	0.3816	0.0396			0.479		
AISI 316L	0.012	0.0158	0.0161	0.0172	0.0111	0.0146	0.0141	0.0144
AISI 317L				0.0062	0.0028		0.0045	0.0045
AISI 904L	0.0013	0.0015	0.0112	0.0102	0.0087	0.0046	0.0094	0.0066

Conclusion

AISI 304L, 316L, 317L and 904L SS were evaluated downstream of the insertion point of the hydrochloric acid solution into the biodiesel and glycerine stream, monitoring points 1 and 2, respectively. AISI 317L presented a noble corrosion resistance at monitoring point 1, presenting an average corrosion rate of 0.0007mm / year, 7 times lower than the rate presented by AISI 316L, and close to the corrosion rate presented by AISI 904L. At monitoring point 2, the AISI 317L steel performed better than AISI 904L, presenting a 52% lower corrosion rate in the average of the campaigns in which they were tested simultaneously.

AISI 317L was selected as pipe material to be used downstream of the insertion point of the hydrochloric acid solution into the biodiesel and glycerine stream, in the biodiesel plant.

Funding

This research was supported by Conselho Nacional de Desenvolvimento Científico e Tecnológico, CNPq, grant number 303735/2015-5.

References

1. Fazal MA, Haseeb ASMA, Masjuki HH (2013) Corrosion mechanism of copper in palm biodiesel. Corros Sci 67: 50-59.
2. Munjur M, Moula E, Nyári J, Bartel A (2017) Public acceptance of biofuels in the transport sector in Finland. Int J Sustain Built Environ 6: 434-441.
3. Wang W, Jenkins PE, Ren Z (2011) Heterogeneous corrosion behaviour of carbon steel in water contaminated biodiesel. Corros Sci 53(2): 845-849.
4. Tian W, Du N, Li S, Chen S, Wu Q (2014) Corros Sci 85: 372-379.
5. Du D, Chen K, Lu H, Zhang L, Shi (2016) Corros Sci 110: 134-142.
6. Delaunois F, Tshimombo A, Stanciu V, Vitry V (2016) Corros Sci 110: 273-283.
7. Feng X, Lu X, Zuo Y, Zhuang N, Chen D (2016) Corros Sci 103: 223-229.
8. Abel J, Virtanen S (2015) Corros Sci 98: 318-326.
9. Li HB, Jiang ZH, Cao Y, Zhang ZR (2009) Metall Mater 16: 517-524.
10. Pistorius PC, Burstein GT (1992) Growth of corrosion pits on stainless steel in chloride solution containing dilute sulphate. Corros Sci 33: 1885-1897.
11. Burstein GT, Mattin SP (1992) A preliminary investigation into the microscopic depassivation of passive titanium implant materials in vitro. Philos Mag Lett 66: 127-131.
12. Burstein GT, Vines SP (2001) Repetitive nucleation of corrosion pits on stainless steel and the effects of surface roughness. Electrochem Soc 148: B504-B516.
13. Fazal MA, Haseeb ASMA, Masjuki HH (2012) Degradation of automotive materials in palm biodiesel. Energy 40: 76-83.
14. Geller DP, Adams TT, Goodrum JW, Pendergrass J (2008) Fuel 87: 92-102.
15. Sgroi M, Bollito G, Saracco G, Specchia S (2005) BIOFEAT: Biodiesel fuel processor for a vehicle fuel cell auxiliary power unit: Study of the feed system. Power Sources 149: 8-14.
16. Haseeb ASMA, X Masjuki HH, Ann LJ, Fazal MA (2010) Fuel Process Technol 91: 329-334.
17. Fazal MA, Haseeb ASMA, Masjuki HH (2010) Comparativ e corrosive characteristics of petroleum diesel and palm biodiesel for automotive materials. Fuel Process Technol 91: 1308-1315.
18. Upadhyay N, Pujar MG, Singh SS, Krishna NG, Mallika C, et al. (2017) Corrosion 73(11): 1320-1334.
19. https://www.nickelinstitute.org/~/media/Files/Presentations/NickelinStainlessSteelsCutlerNewDelhi20111214.ashx